

DESIGN AND EVALUATION OF A STEAMVR TRACKER FOR TRAINING APPLICATIONS – SIMULATIONS AND MEASUREMENTS

Marcin Maciejewski, Marek Piszczek, Mateusz Pomianek, Norbert Palka

Military University of Technology, Institute of Optoelectronics, gen. Sylwestra Kaliskiego, 2, 00-908, Warsaw, Poland
(✉ marcin.maciejewski@wat.edu.pl, +48 261 839 627, marek.piszczek@wat.edu.pl, mateusz.pomianek@wat.edu.pl, norbert.palka@wat.edu.pl)

Abstract

Virtual reality (VR) has become a realistic alternative to conventional learning methods in numerous fields including military training. Accurate and precise tracking of a user wearing a head-mounted display is necessary to achieve an immersive VR experience. The widely available SteamVR system, where licensed users can design and construct trackers optimized for a given application can be an alternative to very expensive professional motion tracking. This paper presents the complete design process of a SteamVR tracker dedicated to a shooting simulation in a VR environment. We describe the optimization and simulation of the tracker's shape and configuration of the sensors. In the simulation phase the developed model had better parameters than its commercial counterparts. Next, the optimized prototype was constructed and configured. The dedicated and automated measuring arrangement provided experimental verification of the tracker's performance. Tracking performance as well as the accuracy and precision of both position and orientation measurements were determined and compared with simulations, which proved that the simulation software can accurately predict selected properties of the proposed tracker.

Keywords: motion capture, SteamVR, accuracy and precision, tracker design, virtual shooting simulator.

© 2020 Polish Academy of Sciences. All rights reserved

1. Introduction

Shooting training for soldiers is expensive due to high prices of modern weapons and ammunition. Therefore, shooting simulators are implemented more and more often to achieve cost reductions and facilitate shooting training. Currently, the most popular shooting simulators are based on laser pointer detection, where a laser is attached to a weapon and the virtual scene is presented on a large screen [1]. In this solution, aiming at targets is accurate and relatively simple. However, during training, the supervisor has only limited possibilities to infer the causes of a trainee's failures unless additional sensors are used in the system. Another problem of simple laser pointer systems is the limitation of their application to small arms and some types of light weapons only. More advanced and expensive systems (*e.g.* the Spartan [2]) can accurately track

the failures made by the shooter and provide training in heavy weapons and missiles. Therefore, a competitive type of simulator was developed, in which *head-mounted display* (HMD) goggles are used instead of large screens while the aiming point is determined by the motion tracking system. In such simulators, the supervisor sees exactly what the trainee does and can identify and correct mistakes made while aiming. In addition, immersive simulators can be also used to train operators of *man-portable air-defense systems* (MANPADS) or similar types of weapons.

Accurate and precise motion tracking systems are required to implement the above-mentioned VR-based simulators. Such systems constitute one of the basic interfaces between a *virtual reality* (VR) environment and its users and are necessary for cooperation with HMDs [3–7]. The position (coordinates x , y , z) and orientation (angles α , β , γ) of a tracked element, collectively referred to as a pose [8], must be associated with the position and orientation of a “camera” from which we observe the virtual world. More advanced systems use motion tracking technology to transfer to the virtual world not only the position of the hands or the whole body of the user but also various elements from the real world, *e.g.* weapon models used in shooting simulators [9].

The impression of immersion, *i.e.* the sense of presence in the virtual world, depends on the type and performance of the tracking system. Any errors and delays in the operation of the tracking not only significantly reduce the impression of immersion but can also cause so-called virtual reality sickness. The type of positioning technology has a significant impact on its price because the value of the elements of some motion tracking systems may constitute the majority of the costs that will be incurred when building virtual reality systems [10].

Commercially available and currently developing positioning systems for VR environments, due to high accuracy required, are often based on optoelectronics [11]. There are more accurate but also more expensive multi-camera systems and less accurate but cheaper single-camera systems. The third group of systems, relatively non-expensive but accurate, is based on the lighthouse method. One of the representatives of this group is the SteamVR tracking system developed by VALVE [12] and used in HTC VIVE devices. Its advantage is openness to licensed users who can design, manufacture and sell their own tracking device designs (called trackers), optimized for a given application. This is important because the results of the work carried out by our team show that parameters of standard commercial SteamVR trackers can be significantly impaired due to the lack of visibility when used to track large objects such as MANPADS. The package of tools provided by VALV is helpful in the tracker design process. It allows users to design an optimal constellation (spatial arrangement) of sensors located on a given tracker surface and simulate the tracking performance of developed models. An important issue is the accuracy of the Steam simulation model because simulations are the essential stage in the sensors’ constellation design algorithm, while the constellation is critical to the tracker’s performance.

This research aims at experimental verification of simulation results obtained with the aforementioned tools for a tracker developed for a shooting simulator and examination of the accuracy and precision of the pose tracking. Research related to SteamVR tracking devices can be found in [13] but it concerns commercial devices only. A similar design process described in [14] does not contain detailed research on the tracking performance of the prepared device. In turn, [15] described the design of a tracker along with the research, but only the hardware components, without the software design support, of the SteamVR system were considered.

The beginning of this paper describes the tracker optimization process for a shooting simulator. Thanks to the SteamVR tracking HDK development package, the optimal shape and configuration of the sensors were determined. Next, housing for the prototype was constructed using 3D printing technology. A dedicated and automated measuring arrangement provided experimental verification of the tracker’s performance. Tracking quality, as well as the accuracy and precision

of both position and orientation measurements, was determined and compared with simulations. The described method is based on similar analyses carried out for the LeapMotion controller [16]. To the best of our knowledge, this type of research has not previously been published for the SteamVR tracking platform.

2. Design and simulations

The SteamVR system uses the lighthouse method to provide the position and orientation of objects thanks to the solution of the so-called *Perspective n Point* (PnP) problem [17]. The system obtains position and orientation data with a set of sensors located on the tracker, which are illuminated by the base station. The base station consists of an LED panel that initially emits a wide synchronization blink and two rotary heads with perpendicular rotation axes emitting narrow laser radiation in the 830 nm range. Detection of the synchronization blink by the sensors begins the countdown of time until the arrival of the pulse from the laser beam sweeping the working area. Knowing the angular velocity of the head and the time after which the photodetector detected the laser pulse, the system determines the angle and, thus, the direction in which the detector is located (Fig. 1a).

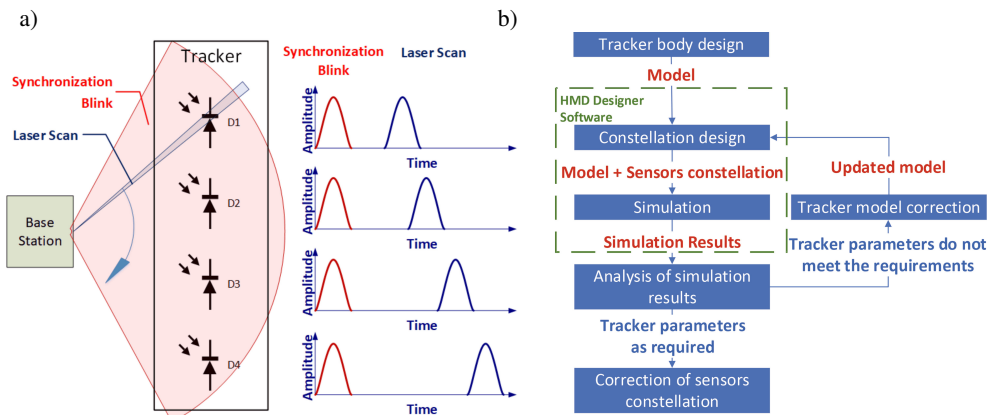


Fig. 1. a) Operating principle of the SteamVR tracking system, b) Algorithm for designing SteamVR devices. Frames indicate the design stages. Red color indicates the results.

The directions of the detectors are the basis for the formulation of the equations for the PnP algorithm. An unambiguous solution of this mathematical problem and, consequently, correct tracking, requires data from at least four sensors which are not located in a single plane (are non-coplanar). One should also consider time jitter which influences the position determination. The jitter results from the clock quantization error with a standard deviation of about 21 ns and the instability of the rotation speed of the base station engines with a standard deviation of 167 ns. To minimize the jitter-related instability, it is necessary to ensure that the distances between the sensors receiving the signal from the base station are as large as possible. To sum up, the requirements can be reformulated as visibility of at least four non-coplanar sensors which are as far apart as possible.

The conditions mentioned above should always be met, regardless of where in the workspace and in which orientation the tracker is located. The design of an optimal tracker shape and

distribution of sensors on it, in a way that fulfills the requirements, is a complicated problem which cannot be solved analytically. Therefore, we used the HMD Designer software which distributes sensors on the surface of the given body in a way that ensures the best tracking and then, through simulation, determines the performance of this tracking. Using the two functions given, the following algorithm for designing SteamVR trackers was proposed (Fig. 1b).

The starting point is to develop a three-dimensional model of the tracked object to which the tracker is attached. So, the pose of the tracker determines the pose of the tracked object. For this task, we used a MANPAD launcher. To correctly imitate the scenario under consideration, the head model of the user with HMD was also loaded into the simulator (Fig. 2a). The initial shape of the tracker at the beginning of algorithm is arbitrarily chosen based on the experience of the designer and some general guidelines. The main clue for the designed objects is that larger objects with a large number of non-coplanar surfaces are tracked better. The tracker itself, the tracked object (the launcher) and the head with mounted goggles can block the radiation reaching the sensors in some poses and, therefore, this should be taken into account in a correct simulation.

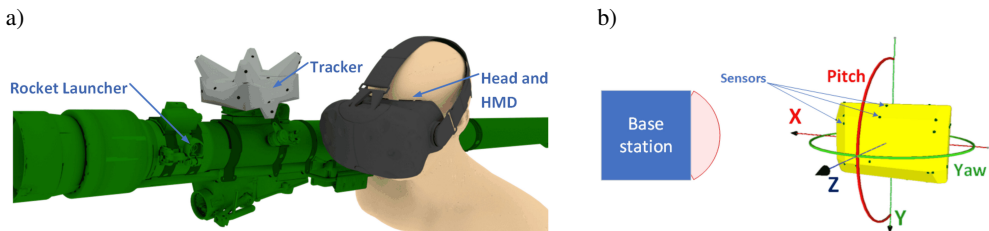


Fig. 2. a) 3D models used in the simulation, b) Rotation of the tracker with sensors during the simulation.

Twenty-four sensors were used in the described project, which is the maximum number for wireless operation. The project's priority is to achieve maximum tracking accuracy, and with large device sizes, so a larger number of sensors allows for better results during the simulation. The cost reduction resulting from limiting the number of sensors is small due to the low unit price of the sensors. In the simplest case, the distribution of sensors on the surface of a given tracker is inserted into the simulator and placed in line with the base station at a given distance (2m by default). Then the model is rotated stepwise around the pitch and yaw axes (Fig. 2b). Implementing a roll rotation is not required because, from the base station's perspective, there is no change in the visible sensors with changes in the roll angle. The software determines which sensors receive signals from the base station at the given orientation which depends on the angle between the sensor and the base station's frontal planes. The software also takes into account the problem of sensor blocking. In the optimization mode, the software randomly distributes sensors on the surface of the given tracker, and then repeatedly rearranges them, checking each time whether the changes have led to improved tracking performance. If so, the resulting constellation becomes the starting point for subsequent sensor rearrangements. Since the software generates several initial constellations, one run of calculations also results in several output constellations. The best one is selected based on its score and an approximate estimation of the tracking performance. Each result contains complete tracking simulation data, which is used to check the fulfillment of the requirements.

Consequently, graphical data about the number of sensors receiving signals from the base station and the predicted error of the tracker's position and orientation are generated. If the results obtained do not meet the requirements, changes to the shape of the tracker should be carried out. The parts of the tracker which require changes are selected on the basis of the simulation data

analysis. The updated model is reloaded into the HMD Designer software and the entire cycle is repeated. The optimization ends when the parameters of the model fulfill the requirements. The last step is manual improvement of those sensors whose position is not physically feasible, e.g. when the software places them too close to the edge of the housing. Figure 3b presents selected shapes of the tracker which are further modifications of one of the initial models used in the optimization process as well as simulation results for all shapes.

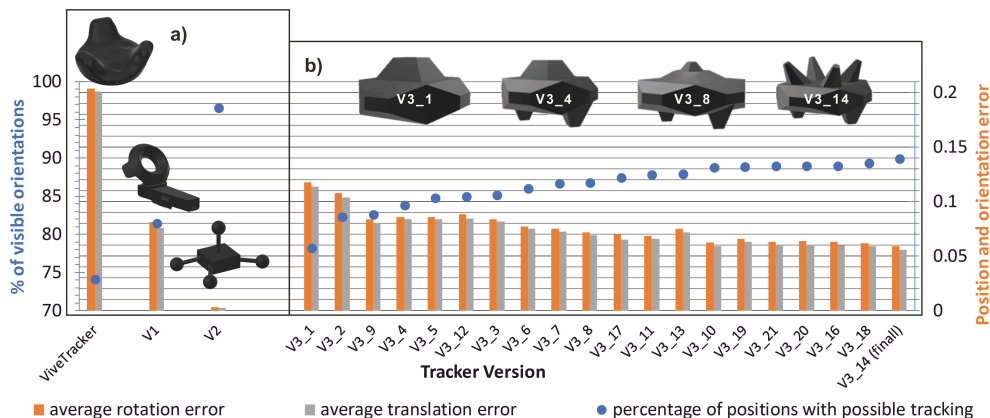


Fig. 3. Comparison of simulation results for commercial (a) and authorial (b) trackers.

Both considered variants (V2 and V3) at the simulation stage have better parameters than their commercial counterparts which confirms the need for the design of the optimized tracker. V2 has the best parameters – it is tracked in more than 95% of positions with the lowest error, due to significant spatial separation of the sensors. However, V3 which had slightly worse parameters was selected for further practical implementation due to its higher mechanical stability.

3. Construction of the tracker

The prototype housing with mounting points for sensors, electronic boards, connectors and buttons was developed based on the shape of the V3 model. The work was carried out in SolidWorks and the model prepared for 3D printing is shown in Fig. 4a. The electronic components included in the tracker’s construction are part of the SteamVR tracking HDK package currently produced by Triada Semiconductors. These include a controller containing the following modules: timers implemented in the FPGA, wireless and USB communication, a power supply controller, 6 DOF IMU (accelerometer and gyroscope) and a microcontroller monitoring the device operation. In addition to the controller, 24 sensor modules were installed in the device. Each of them consists of a PIN photodiode and an ASIC TS4231 module responsible for conditioning the received signal.

The elements of the tracker housing were made by 3D printing from ABS material. The device was then assembled and the sensors were precisely located in the internal housing sockets (Fig. 4b). Next, the device was configured thanks to the JSON configuration file and calibrated. Finally, preliminary tests proved that the prototype was correctly detected by the SteamVR system and the constituent sensors received signals from the base station. The developed model may seem large, but its size is justified by the size of the launcher (length about 2 m, diameter over 70 mm)



Fig. 4. The lower part of the tracker model prepared for printing: with electronic components (a); photo of the tracker prototype (b) and its dimensions (units – mm) (c).

for which it was designed. The 3D models (Fig. 2a) with the final version of the tracker proved that the tracker does not disturb the user during shooting. The mass of the tracker equals 0.5 kg and is negligible as the mass of the launcher set exceeds 16 kg.

4. Experimental setup

In order to validate the simulation tools, the operation of the simulator was reproduced in laboratory conditions. The tracker was placed in line with the base station at the distance of 2 m. The measuring setup provides the possibility of changes in the orientation of the tracker in a way that reflects the changes used in the simulator. This means the changes in rotation are in a fixed sequence while maintaining the same position. For each of the examined tracker orientations, the number of sensors was determined which was able to correctly register signals from the base station. To ensure the most accurate representation of simulation conditions, the room in which the measurement was performed was free from objects and surfaces that could cause reflections.

An LR Mate 200iD/4s industrial robot arm with a R-30iB Mate controller was used to construct the measuring setup. The robot has a positioning repeatability of 0.01 mm. In addition, thanks to the use of the so-called tool coordinate system, the position of the tracker's center remained constant during orientation changes. Due to the limited load capacity of the robot head (4 kg), the tests and simulations were carried out for the tracker itself without the obscuring objects.

The tracker was fitted with a Picatinny rail mount (STANAG 2324). Two assembly adapters were prepared to install the mount on the robot head. One was the standard Picatinny rail mounted on the robot head. The other attachment was used to mount the tracker on the robot after being turned by 180 degrees. This procedure minimized the effect of obstruction of the tracker by the robot arm during measurements for pitch angles between 0 and 90 degrees.

The robot and the base station were placed in a laboratory room with walls covered with diffusing material to reduce signal reflections. The robot arm itself was also covered with similar material. For accurate placement of the robot and the base station in the room, a precise Optitrack motion tracking system was used, with measurement uncertainty below 1 mm. The arrangement of the measuring setup elements is shown in Fig. 5a.

In order to automate the measurement process, control and data acquisition software was prepared which consisted of proprietary library packages prepared in C# for robot control and data acquisition from the SteamVR system as well as software running on the robot controller. The LabView environment was chosen to integrate the prepared libraries due to the ease of implementation of algorithms with the user interface. The software provides two types of measurements:

1. Acquisition of data from individual sensors including the number assigned to a given sensor, the number of signals registered by the sensor, the angle describing the position at which the sensor is located, and the standard deviation of the determined angle. The results are given independently for vertical and horizontal scanning and separately for each sensor. Data acquisition for each tracker orientation is performed for a set period of time (10 s). The synchronization flash is generated at a frequency of 60 Hz. Therefore, illuminated sensors should register about 600 signals at this time (300 for both vertical and horizontal scans). It is assumed that the sensor is considered illuminated if it has registered at least 100 signals from each scan.
2. Acquisition of data generated by the SteamVR engine, *i.e.* the position and orientation of the tracker. For each orientation of the robot head, which, as in the measurement series described above, moves in the simulator-like manner, multiple measurements are made (10,000 times). The measurement results are: three components of the tracker position and three components of the tracker orientation. Based on the analysis of the results obtained, the precision of the position and orientation measurements can be determined depending on the tracker's orientation relative to the base station.

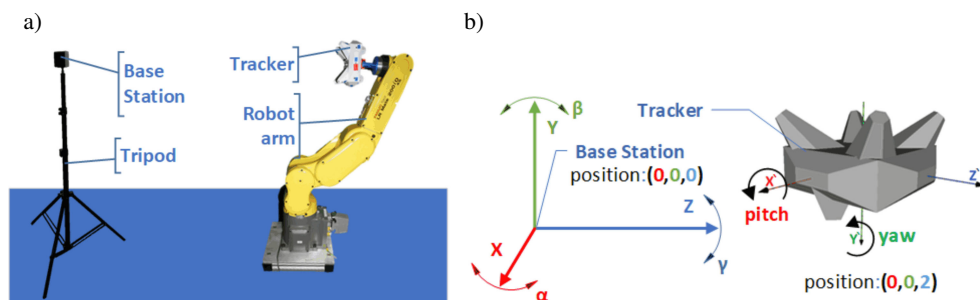


Fig. 5. Scheme of the measuring setup (a). Coordinate system for the position of the tracker during measurements (b).

The measuring software is equipped with a graphic interface presenting the results in real-time, which is important because the measurements are time-consuming (several or even tens of hours). Therefore, it is important to be able to check ongoing measurements for errors that may have occurred, *e.g.* due to noises.

The evaluation of the position and orientation data of the tracker determined by the Steam engine requires a prior definition of the coordinate system. In the described case, measurements were carried out for the system with the uncalibrated workspace. This means that the coordinate system origin was located in the geometric center of the SteamVR base station. The devices used a left-handed coordinate system. From the perspective of the user in front of the base station, the “X” axis is directed to the left, the “Y” axis is upwards and the “Z” axis is from the base station toward the user. The position of the tracker located in front of the base station in one line, at a distance of 2 m should be (0, 0, 2) (Fig. 5b).

The above data is supplemented with information on the local coordinate system of the tested device. The term tracker position means the position of the origin of its local coordinate system (X' , Y' , Z'). This system is used to determine the orientation of the tracker. It is calculated as the rotation between the global coordinate system and the local system of the tracker (angles α , β , γ). The left-hand system was also used in the studied case. Its origin is located in the geometric center of the tracker.

5. Results and discussion

5.1. Number of sensors receiving the signal from the base station

Data collection using the software described above, regarding individual sensors receiving a signal from the base station, was performed with an angle step of 2 degrees and lasted 75 hours. The measurement was carried out twice and the correlation coefficient between them was 0.93, which indicates high repeatability. The experimental results regarding the number of visible sensors (Fig. 6b) were then compared with the previously described simulation (Fig. 6a). Generally, the results are similar, as evidenced by the correlation coefficient of 0.588. In addition, in both results, the smallest number of tracked sensors (6) is higher than the minimum number of the sensors required for proper tracking (4). The correct location of the sensors (large distances and non-coplanarity) was ensured at the design stage and confirmed by the simulation results presented in a further part of the work (Fig. 9a and Fig. 11a).

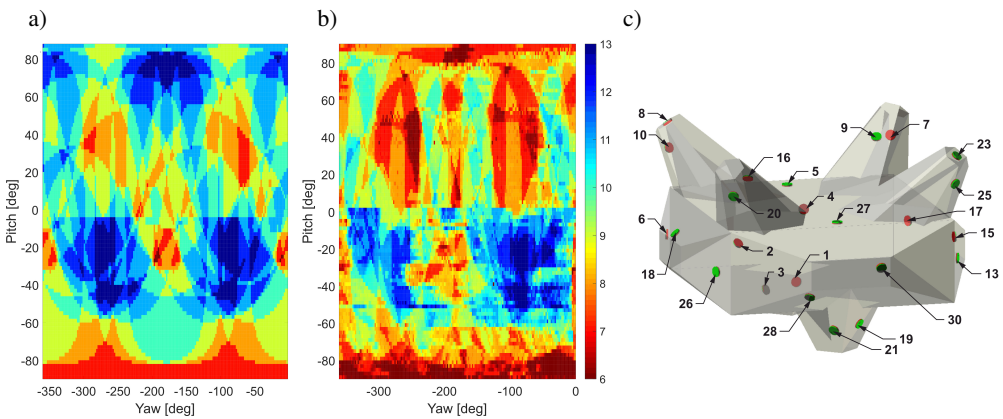


Fig. 6. Number of sensors receiving the signal from the base station: simulation (a) and measurements (b). The Z axis represents the number of visible sensors. Sensor locations and numbers (c).

To understand the differences between the measurements and the simulation, additional analyses were made regarding the visibility of individual sensors (Fig. 6c). It turned out that for 17 sensors the correlation coefficient between the measurements and the simulation is over 0.6 (Fig. 7). However, a negative correlation value was noted for two of the analyzed sensors.

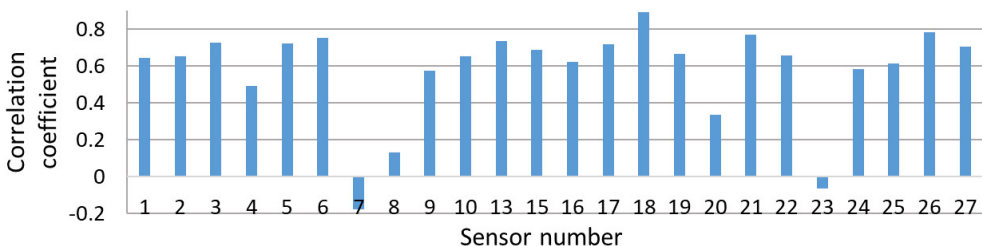


Fig. 7. The correlation coefficients between the measurement and simulation results for individual sensors. Due to technical issues, the sensors are not numbered consecutively.

Additionally, Fig. 8 shows the comparison of charts showing the simulation and experimental visibility of selected sensors for three correlation coefficient cases: high ($r = 0.9$), medium ($r = 0.7$), and negative ($r = -0.2$). An in-depth data analysis revealed that there are orientations when the sensor receives a signal that according to the simulation should not be received. The reason is probably a reflected signal of unknown origin. For these cases, the standard deviation of the sensor orientation is three orders higher than for orientations with normal visibility.

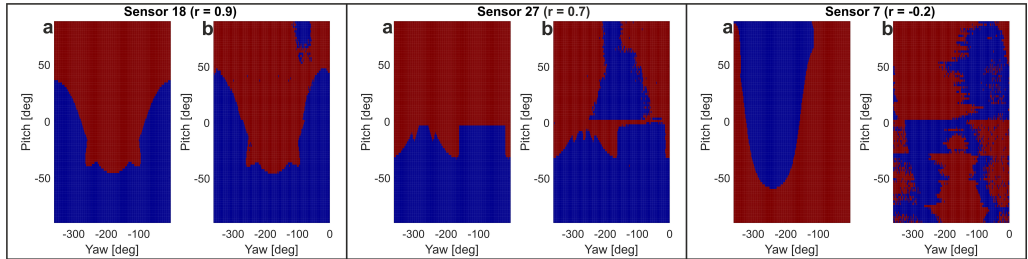


Fig. 8. Comparison of measurements (a) and simulation (b) data for selected sensors. The blue color represents the orientation in which the sensor receives the signal; the red color represents the orientation in which the signal is not received.

5.2. Accuracy and precision of position determination

The problem of precision and accuracy of measurements was analyzed separately. Precision is generally understood as the stability of orientation determination and is calculated as standard deviation of data collected at a given point, determined separately for each of the components (X, Y, Z), according to (1):

$$S_{q_j} = \sqrt{\frac{1}{N-1} \sum_{i=1}^N (Q_{ij} - \mu_{q_j})^2}, \quad \text{where: } \mu_{q_j} = \frac{1}{N} \sum_{i=1}^N Q_{ij}, \quad (1)$$

where: $S_{q_j} = S_{x_j}, S_{y_j}, S_{z_j}$ are standard deviations of individual position components at a given point (the measurement precision of individual components), $\mu_{x_j}, \mu_{y_j}, \mu_{z_j}$ substituted for μ_{q_j} are the average values of individual position components, X_{ij}, Y_{ij}, Z_{ij} substituted for Q_{ij} are the matrices containing the measurement results for a given position component, i is the index related to the measurement number at a given measuring point (in a given position of the robot head), j is the index related to the measuring point number, and N is the number of measurements at a given point.

The global position precision at a given measuring point is the root mean square (RMS) value (S_j) determined for the individual components:

$$S_j = \sqrt{\frac{S_{x_j}^2 + S_{y_j}^2 + S_{z_j}^2}{3}}. \quad (2)$$

The Euclidean distance (E_j) between the expected position and the position determined by the system was used to obtain accuracy:

$$E_j = \sqrt{(\mu_{x_j} - x_r)^2 + (\mu_{y_j} - y_r)^2 + (\mu_{z_j} - z_r)^2}, \quad (3)$$

where: x_r, y_r, z_r are the actual values of the individual components.

Figure 9a shows the position measurement error obtained from the simulation carried out in the same way as for the sensor number analysis (Fig. 5b). The simulation software does not accurately describe the causes of the errors, so the plot can only be used for qualitative analysis. Figures 9b–c show S_j and E_j determined based on (2) and (3), respectively.

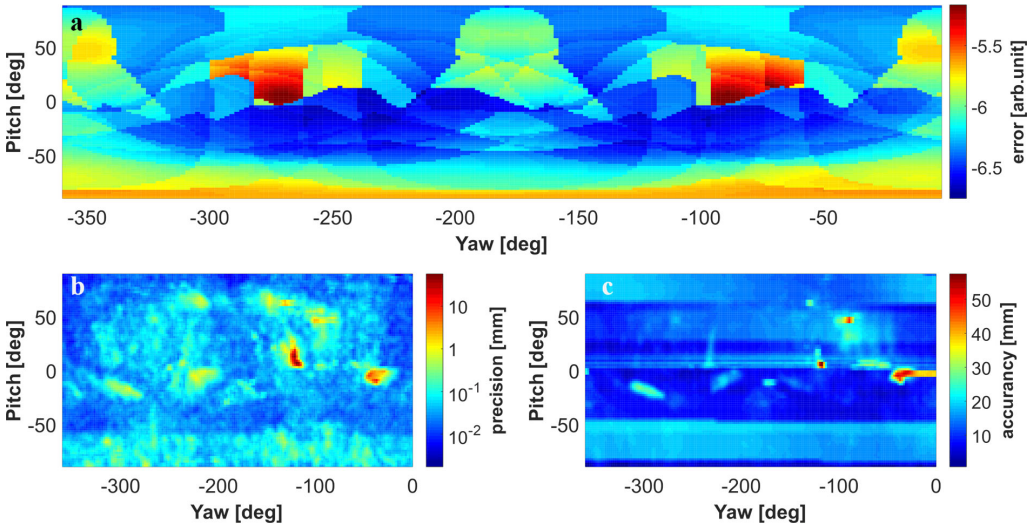


Fig. 9. Simulation-based position errors (a). Precision (b) and accuracy (c) of the experimental position determination.

The position measurement precision determined for the tested prototype does not exceed 1 mm for over 97% of the inspected orientations. A similar percentage of the tested orientations had an accuracy of less than 20 mm. The tracker kept tracking throughout the measurement period and only in three selected orientations had higher accuracy values and worse precision.

The experimentally-obtained precision and accuracy results do not coincide with the simulation data (the correlation coefficient equal to 0.1). The simulator shows only theoretical errors calculated from the PnP algorithm (Fig. 9a), while experimental values (Fig. 9b, c) can also result from other factors such as reflections and imprecise sensor placement.

The graph above presents a summary of average values of individual components of the location. However, these charts do not contain information about the impact of individual components on the accuracy and precision of the results. Therefore, the analyzes shown above are supplemented by charts containing values of standard deviations and absolute measurement accuracy for individual axes (Fig. 10).

As expected, the Z axis data has the largest standard deviation and the largest accuracy values. Like any motion tracking system based on the PnP solution, SteamVR tracking least accurately determines the distance between the base station and the tracker which corresponds to the Z coordinate of the tracker's position. Moreover, the accuracy and precision of the position measurements on this axis depend strictly on the precision of sensor placement, according to the data contained in the configuration file. The areas with higher values appearing at several points in Fig. 10c and f may suggest that the positions of at least several sensors differ from the ones assumed at the design stage. The reason may be inaccurate housing construction during the process of 3D printing.

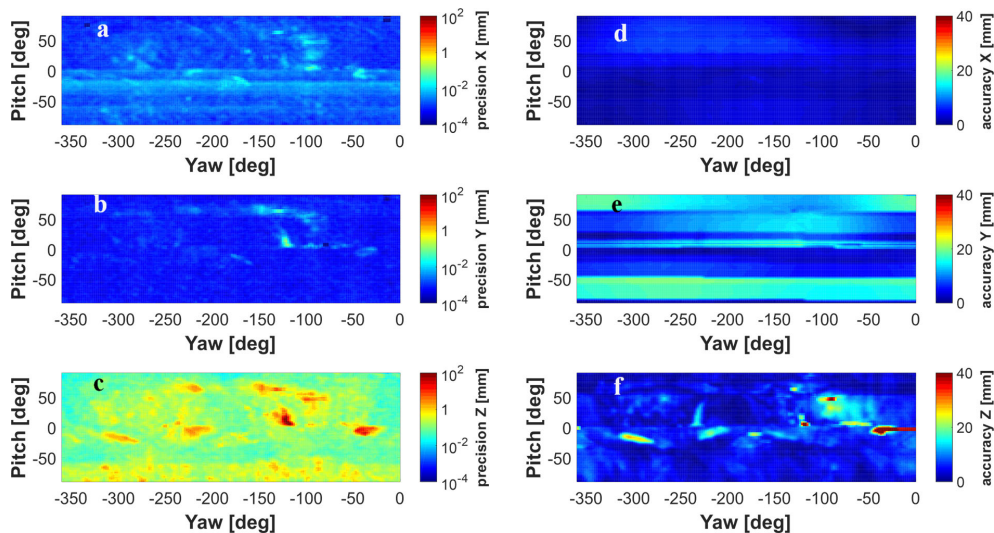


Fig. 10. Precision (a–c) and accuracy (d–f) of the measurements for individual position components.

5.3. Accuracy and precision of orientation determination

The precision of orientation was determined as standard deviation from the measurement series at a given point independently for each of the rotation axes using (1), where S_{α_j} , S_{β_j} , S_{γ_j} substituted for S_{q_j} are standard deviations of individual orientation components at a given point (measurement precision of individual components), μ_{α_j} , μ_{β_j} , μ_{γ_j} substituted for μ_{q_j} are average values of individual orientation components and A_{ij} , B_{ij} , Γ_{ij} substituted for Q_{ij} are the matrices containing the measurement results for a given orientation component. As to the global orientation precision (S_{r_j}), the RMS value of individual components of the tracker's orientation was adopted in accordance with (4):

$$S_{r_j} = \sqrt{\frac{S_{\alpha_j}^2 + S_{\beta_j}^2 + S_{\gamma_j}^2}{3}}. \quad (4)$$

The accuracy of the orientation measurement for individual axes was also determined analogously to the measurement of position components as the difference between the measured and the set value. However, some difficulties are posed by the analysis of the total accuracy of the orientation measurement because explicit determination of the angular shift between the measured and real orientation for Euler angles is ambiguous. Theoretically, it is possible to convert the obtained values to *e.g.* quaternions and determine the angular displacement. However, it was considered that sufficient accuracy would be provided by the RMS value (E_{r_j}) of individual components of the measurement accuracy. The value of the total orientation accuracy in the presented analysis was determined according to (5):

$$E_{r_j} = \sqrt{\frac{(\mu_{\alpha_j} - \alpha_{r_j})^2 + (\mu_{\beta_j} - \beta_{r_j})^2 + (\mu_{\gamma_j} - \gamma_{r_j})^2}{3}}, \quad (5)$$

where α_{r_j} , β_{r_j} , γ_{r_j} are the actual values of individual orientation components at a given point. The results of the analysis of data on the precision and accuracy of the orientation measurements were compared with the data from the simulation (Fig. 11).

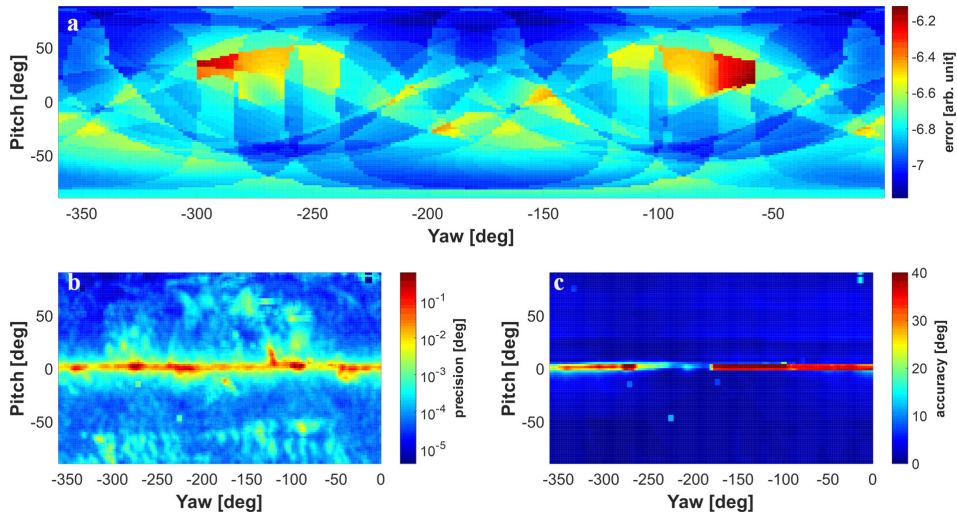


Fig. 11. Simulation-based orientation errors (a). Precision (b) and accuracy (c) of the experimental orientation determination.

The measurement results, do not coincide with the simulation results, having a correlation coefficient of about 0.1. The reasons are probably analogous to those for the position data, *i.e.* the predominance of errors caused by factors other than incorrect sensor placement. Figure 12 presents the contribution to precision and accuracy made by individual components. It can be concluded that the rotation angle α corresponding to the rotation around the X axis was measured precisely and accurately (Fig. 12a, d). Two other components (β and γ) feature very similar characteristics of precision and accuracy (Fig. 12b vs. c and e vs. f) reaching a maximum for pitch angles close to 0 degrees. The reason for this may be problems in the tracking of the device due to the fact that sensors are not mounted accurately enough.

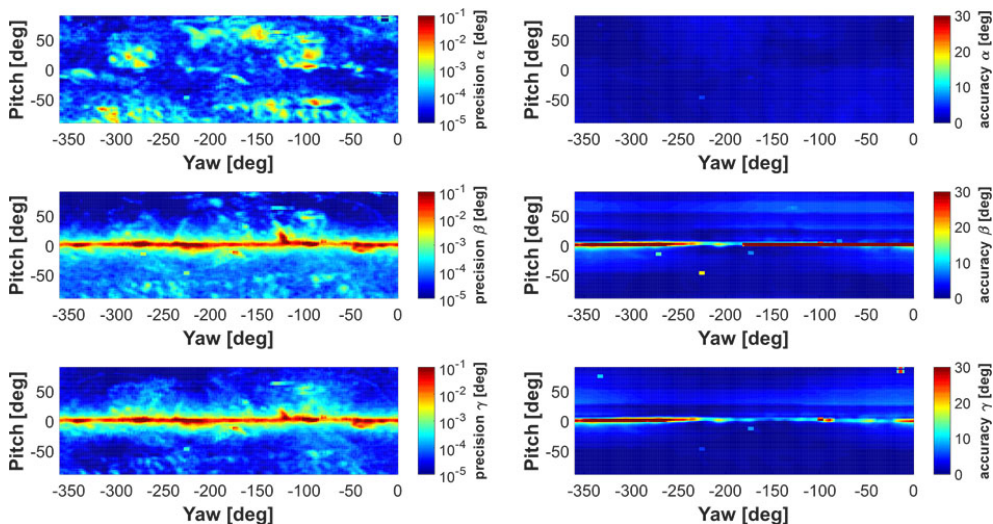


Fig. 12. Precision (a–c) and accuracy (d–f) of the measurements for individual orientation components.

6. Conclusions and future work

This paper presents the results of optimization, simulation, design, construction and experimental verification of a virtual reality tracker for a shooting simulator in a SteamVR environment. The experimental results have proved that the simulation software can accurately predict the number of visible sensors in the designed tracker. However, this regularity does not refer to results regarding the accuracy and precision of both the position and orientation measurements. The first less probable explanation is that the simulation software does not accurately calculate errors for the arbitrary shape of the trackers. An alternative and, according to the authors, more likely explanation is the existence of other factors causing problems with the tracking, like inaccurate sensor placement or reflection-related errors. These factors are probably not taken into account in the ideal conditions of the simulation. The second explanation is supported by the fact that the position measurement precision is worse than that in the SteamVR system specification, which in turn may indicate that the tracker construction is not quite accurate.

The results of accuracy and precision measurements of the developed tracker have shown that for most of the tested orientations, the tracker behaves correctly, *i.e.* the position precision was better than 1 mm, while the orientation precision was better than 0.1 degree. However, some values outside these ranges indicate irregularities in the device's construction. The results above were obtained for the operation with a single base station solely to reproduce the operation of the simulator. In normal operating conditions with calibrated space and two base stations, the performance of the tracker under consideration can be even better. Tests to determine whether accuracy and precision values higher than those declared in the specification can also occur for this configuration will be the subject of our future work. Our future research will focus on determining whether the accuracy and precision fulfill the requirements in all positions and orientations in real conditions.

References

- [1] Soetedjo, A. & Nurcahyo, E. (2011). Developing of Low Cost Vision-Based Shooting Range Simulator. *IJCSNS International Journal of Computer Science and Network Security*, 11(2) 109–113. <http://eprints.itn.ac.id/3192/>
- [2] Glogowski, T. Hłosta, P. Stepniak, S. & Swiderski W. (2017). Optoelectronics applications in multimedia shooting training systems: SPARTAN. *Proceedings of SPIE Security + Defence*, Poland. <https://doi.org/10.1117/12.2277002>
- [3] Fung, J., Richards, C. L., Malouin, F., McFadyen, B. J. & Lamontagne, A. (2006). A treadmill and motion coupled virtual reality system for gait training post-stroke. *CyberPsychology & Behavior*, 9(2), 157–162. <https://doi.org/10.1089/cpb.2006.9.157>
- [4] Chan, J. C., Leung, H., Tang, J. K., & Komura, T. (2010). A virtual reality dance training system using motion capture technology. *IEEE Transactions on Learning Technologies*, 4(2), 187–195. <https://doi.org/10.1109/TLT.2010.27>
- [5] Hilfert, T. & König, M. (2016). Low-cost virtual reality environment for engineering and construction. *Visualization in Engineering*, 4(1). <https://doi.org/10.1186/s40327-015-0031-5>
- [6] Bogatinov, D., Lameski, P., Trajkovic, V., & Trendova, K. M. (2017). Firearms training simulator based on low cost motion tracking sensor. *Multimedia Tools and Applications*, 76(1), 1403–1418. <https://doi.org/10.1007/s11042-015-3118-z>
- [7] Gourlay, M. J. & Held, R. T. (2017). Head-Mounted-Display Tracking for Augmented and Virtual Reality. *Information Display*, 33(1) 6–10. <https://doi.org/10.1002/j.2637-496X.2017.tb00962.x>

[8] Mihelj, M., Novak, D. & Beguš, S. (2014). Degrees of Freedom, Pose, Displacement and Perspective. In *Virtual Reality Technology and Applications*, 68, 17–34. https://doi.org/10.1007/978-94-007-6910-6_2

[9] Harvey, C., Selmanovic, E., O'Connor, J. & Chahin, M. (2018). Validity of virtual reality training for motor skill development in a serious game. *Proceedings of 10th International Conference on Virtual Worlds and Games for Serious Applications (VS-Games)*, Germany. <https://doi.org/10.1109/VS-Games.2018.8493447>

[10] Anthes, C., Wiedemann, M. & Kranzlmüller, D. (2016). State of the Art of Virtual Reality Technology. *Proceedings of IEEE Aerospace Conference*, United States. <https://doi.org/10.1109/AERO.2016.7500674>

[11] van der Kruk, E. and Reijne, M. M. (2018). Accuracy of human motion capture systems for sport applications; state-of-the-art review. *European Journal of Sport Science*, 18(6) 806–819. <https://doi.org/10.1080/17461391.2018.1463397>

[12] Yates, A., & Selan, J. (2019). *Positional tracking systems and methods* (U.S. Patent No. 10,338,186). U.S. Patent and Trademark Office. <https://patents.google.com/patent/KR20170106301A/en>.

[13] Niehorster, D. C., Li, L. & Lappe, M. (2017). The accuracy and precision of position and orientation tracking in the HTC vive virtual reality system for scientific research. *I-Perception*, 8(3). <https://doi.org/10.1177/2041669517708205>

[14] Ng, A. K. T., Chan, L. K. Y. & Lau, H. Y. K. (2017). A low-cost lighthouse-based virtual reality head tracking system. *Proceedings of International Conference on 3D Immersion (IC3D)*, Belgium. <https://doi.org/10.1109/IC3D.2017.8251910>

[15] Sommer, B. B., Weisenhorn, M., Ernst, M. J., Meichtry, A., Rast, F. M., Kleger, D., Schmid, P., Lünenburger, L. & Bauer, C. M. (2019). Concurrent validity and reliability of a mobile tracking technology to measure angular and linear movements of the neck. *Journal of Biomechanics*, 96, 109340. <https://doi.org/10.1016/j.jbiomech.2019.109340>

[16] Weichert, F., Bachmann, D., Rudak, B., & Fisseler, D. (2013). Analysis of the accuracy and robustness of the leap motion controller. *Sensors*, 13(5), 6380–6393. <https://doi.org/10.3390/s130506380>

[17] Zheng, Y., Kuang, Y., Sugimoto, S., Astrom, K. & Okutomi, M. (2013). Revisiting the PnP problem: A fast, general and optimal solution. *Proceedings of the IEEE International Conference on Computer Vision*, USA, 2344–2351. <https://doi.org/10.1109/ICCV.2013.291>



Marcin Maciejewski obtained the B.Sc. and M.Sc. degree in electronics from the Military University of Technology (MUT) Warsaw Poland in 2014 and 2015, respectively. He is currently pursuing the Ph.D. degree in the field of automatics, electronics and electrotechnology. His current research interests include optoelectronics technologies in virtual reality especially in the field of motion capture systems.



Mateusz Pomianek received a B.Sc. in Mechatronics (2016) and M.Sc. in Optoelectronics (2017) from the Military University of Technology (MUT). He is currently pursuing the Ph.D. degree in the field of automatics, electronics and electrotechnology. His research activity focuses on optoelectronic technologies in virtual reality systems and natural user interfaces.



Marek Piszczek received the Ph.D. degree from Military University of Technology, Poland, in 2000. He is currently Assistant Professor at the same university. He has authored or co-authored 6 monograph, 90 articles, 3 patent applications. His current research interests include engineering of image information in research and application terms: active imaging, machine vision, virtual and augmented reality.



Norbert Palka received the D.Sc. and Ph.D. degrees in electronics, both from the Military University of Technology (MUT) in 2016 and 2004, respectively. In 1999 he received master's degrees in physics, also from the MUT. In 1999, he joined the Institute of Optoelectronics as a researcher. Currently, he holds the positions of the associate professor. His interests have been in various security sensors and optoelectronics. He is the author and co-author of many publications in the

field of security, optoelectronics and terahertz technology.